Original Paper

Capillary Electrophoretic Characterization of Platinum and Silver Nanoparticles in Aqueous Solution Prepared by a Solution Plasma Process

Toshio TAKAYANAGI[*1], Taiki HIROSE[2], Hitoshi MIZUGUCHI[1], Hirotaka OKABE[3], Naoki MATSUDA[3]

[1]*Graduate School of Technology, Industrial and Social Sciences, Tokushima University, 2-1 Minamijosanjima-cho, Tokushima 770-8506, Japan*

[2]*Graduate School of Science and Technology for Innovation, Tokushima University, 2-1 Minamijosanjima-cho, Tokushima 770-8506, Japan*

[3]*Sensing System Research Center, National Institute of Advanced Industrial Science and Technology, 807-1 Shukumachi, Tosu 841-0052, Japan*

Abstract

Aqueous solutions of platinum nanoparticles (PtNP) and silver nanoparticles (AgNP) were prepared by a solution plasma process in the presence of hydrogen peroxide. Both nanoparticle solutions did not show visible-range photo-absorption by surface plasmon resonance, and capillary zone electrophoresis (CZE) was utilized for the characterization of the nanoparticles. An anionic broad peak was detected with the PtNP by the CZE analysis, whereas both an anionic and an electrically neutral peaks were detected with the AgNP. Serious shot signals attributed to the agglomerate of the nanoparticles were not detected with either the PtNP or the AgNP, and the nanoparticles were stably dispersed in an aqueous solution for at least a few tens of week. Dispersion stability of the nanoparticles was also evaluated in salt solutions, as well as with ethanol co-solvent.

Keywords: Platinum nanoparticles; Silver nanoparticles; Capillary zone electrophoresis; Solution plasma process

1. Introduction

Nanoparticles consisted of noble metal are useful in labeling and detection of biogenic substances (gold nanoparticles, AuNP) [1], catalysis (platinum nanoparticles, PtNP) [2], and antibacterial (silver nanoparticles, AgNP) [3,4]. The nanoparticle solutions are also useful substrates for surface-enhanced Raman spectroscopy (SERS) [5]. Characterization of nanoparticles is essential for their utilization and functionalization. Shape analysis of nanoparticles is mainly made by electron microscopy including scanning electron microscope and transmission electron microscope (TEM). Size characterization of nanoparticles in a solution is also made by dynamic light scattering. Capillary zone electrophoresis (CZE) is an alternative to monitor the dispersion of the nanoparticles in an aqueous solution [6-9]. Shot signals are often detected with aggregated/agglomerated nanoparticles, while broad peaks are detected with dispersed nanoparticles based on their wide variations in size and shape [8,9]. CZE was utilized for the characterization of AgNP synthesized with natural products of honey or glucose [10]. Detection sensitivity of AgNP was developed by on-line concentration of AgNP using the reversed electrode polarity stacking mode [11]. Thiol ligands were utilized for the characterization of citrate-capped AuNP and AgNP [12]. Poly(glycidyl methacrylate)-coated AgNP was used for the CZE separation of microspheres [13] and poly(ethylene oxide)-coated AgNP for proteins [14]. Citrate or polymer coated AgNP were

[*]Corresponding author: Toshio TAKAYANAGI
Tel: +81-88-656-7409; Fax: +81-88-656-7409
E-mail: toshio.takayanagi@tokushima-u.ac.jp

resolved by capillary electrophoresis, and ICP-MS detection helped the characterization of the size of AgNP [15]. Size resolutions of PtNP [16] and AgNP [17,18] have been reported by capillary electrophoresis-inductively coupled plasma mass spectrometry (CE-ICPMS). Because the electrophoretic mobility is proportional to the net charge, *i.e.*, the surface area of the nanoparticle, $4\pi r^2$, and inversely proportional to the radius of the nanoparticle, r^{-1}, and therefore, electrophoretic mobility of nanoparticles is proportional to the radius of the nanoparticle [16]. Coupling of ICPMS to the CE separation is also useful for the speciation of Ag between Ag^+ and AgNP [19,20]. Sodium dodecyl sulfate was also utilized for the size/shape separation of AgNP [18,21]. AgNP was also utilized in CZE as a SERS substrate by in-line coupling of CZE to TLC plate [22] and on-capillary detection [23,24].

Two of the present authors (N. M. and H. O) have established the facile synthesis of nanoparticles by a solution plasma (SP) process; AuNP [25-28] and PtNP [29,30] were successfully prepared. The nanoparticle solutions prepared by the SP process are stabilizer free, and the nanoparticles thus prepared have been subjected to the SERS platform [26,27] and direct electron transfer reaction of redox protein [28]. Dispersion stability of the AuNP prepared by the SP process was evaluated through CZE by the present authors in the absence of any stabilizer [31].

In this study, aqueous solutions of PtNP and AgNP were prepared by the SP process, and they were characterized by CZE; the dispersion stability in an aqueous solution was investigated, as well as in NaCl solutions and with ethanol cosolvent.

2. Material and methods

2.1. Apparatus

An Agilent Technologies (Waldbronn, Germany) ^{3D}CE equipped with a photodiode array detector was used as a CZE system. A fused silica capillary purchased from GL Sciences (Tokyo, Japan) was cut in an adequate length and it was packed in a cassette cartridge; the cartridge was installed in the CZE system. Dimensions of the separation capillary were 75 μm i.d., 375 μm o.d., 48.5 cm in total length, and 40 cm in effective length from the injection end to the detection point. A ChemStation software (Agilent Technologies, Ver. B04.02) was used for the control of the CZE system and the data analysis. A Horiba (Kyoto, Japan) F-71s pH meter was used for adjusting the pH of the separation buffers.

A Transmission Electron Microscope JEM-2100F (JEOL, Tokyo, Japan) was used for taking TEM images of the nanoparticles. The applied voltage of the electron gun was 200 kV, and the image resolution was 0.23 nm as the particle size.

Absorption spectra of the nanoparticle solutions were measured by a JASCO (Tokyo, Japan) V-630 Spectrophotometer with 1 cm pathlength quartz cells.

2.2. Chemicals and reagents

Separation buffer components of 2-(*N*-morpholino)ethanesulfonic acid (MES), 2-[4-(2-hydroxyethyl)piperazin-1-yl]ethanesulfonic acid (HEPES), and *N*-cyclohexyl-2-aminoethanesulfonic acid (CHES) were purchased from Dojindo Laboratories (Kumamoto, Japan). Other reagents were of analytical grade. Water used was purified by a Milli-Q Gradient A10 (Merck Millipore, Billerica, MA, USA).

Solutions of PtNP and AgNP were prepared by the SP process as the same manner previously reported [25-30]. Typically, a 50 mL Pyrex beaker was used as an SP processing reaction cell. A couple of Pt (20 cm long, 2 mm ϕ, 99.99%, Tanaka Kikinzoku Kogyo K.K., Tokyo, Japan) or Ag (20 cm long, 2 mm ϕ, 99.99%, Tanaka Kikinzoku Kogyo K.K., Tokyo, Japan) electrodes were set with an angle of 30 degrees to the perpendicular direction into the SP reaction cell and the gap between them were kept at 0.5 mm. An aqueous solution of 5.0 %(w/w) H_2O_2 was poured into the reaction cell. A high voltage bipolar pulsed power supply (MPS-06K-01C, KURITA Seisakusho, Kyoto, Japan) was used as a power source. The applied bipolar voltage, the pulse width, and the frequency were 2.0 kV, 2.5 μsec, and 20 kHz, respectively. The energization period was set at 5 min.

2.3. Procedure for CZE measurements

A separation buffer was prepared with 10 mmol L^{-1} CHES with its pH adjusted at 9.2 with NaOH. The buffer component was chosen based on the fast electroosmotic flow and fast detection of the nanoparticles. After the separation capillary being filled with the separation buffer, the PtNP or the AgNP solution was injected into the capillary from the anodic end by applying pressure of 50 mbar for 3 s. Both ends of the capillary were dipped in each buffer vial, and a DC voltage of 20 kV was applied to the capillary for the electrophoresis. The PtNP or the AgNP were photometrically detected at 220 nm. During CZE, the capillary cartridge was thermostat at 25 °C by circulating constant temperature air. Effective electrophoretic mobility (μ_{ep}) of the nanoparticles was calculated as in a usual manner. Even when the additive, such as salt solution or ethanol, was added to the nanoparticle solutions, the dilution factor of the nanoparticle solutions was less than twice.

3. Results and discussion

3.1. Characterization of the PtNP and the AgNP by TEM and UV-vis spectrophotometry

The PtNP and the AgNP prepared by the SP process were directly evaluated by TEM. Typical TEM images are shown in Fig. 1. Because the nanoparticle solutions were dried on a grid mesh before the TEM measurements, images of the

nanoparticles were taken as agglomerates. It is noted from Fig. 1(a) that the PtNP consists of *ca.* 2 nm particles. The particle size agreed with our previous study, an average diameter of 3.3 nm [30]. On the other hand, the AgNP were taken as dispersed particle size as in Fig. 1(b); the particle size is distributed around 1-10 nm. Both nanoparticles were successfully prepared.

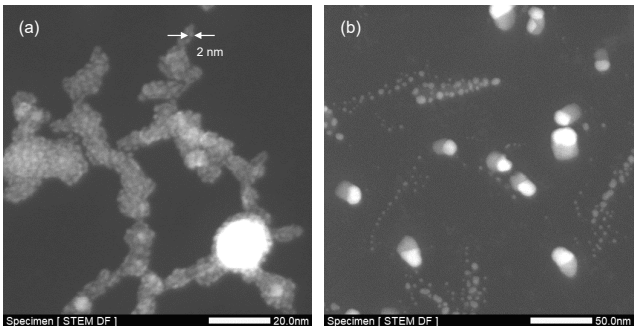

Fig. 1. TEM images of (a) PtNP and (b) AgNP.

Nanoparticle solutions have traditionally been evaluated through the visible-range absorption spectrophotometry with the surface plasmon resonance. However, the AgNP and the PtNP prepared by the SP process are colorless in the visible range, and any peak of the plasmon resonance was not observed, as shown in Fig. 2. The spectrophotometric results directed us to the separation analysis of the nanoparticles by CZE with UV photometric detection.

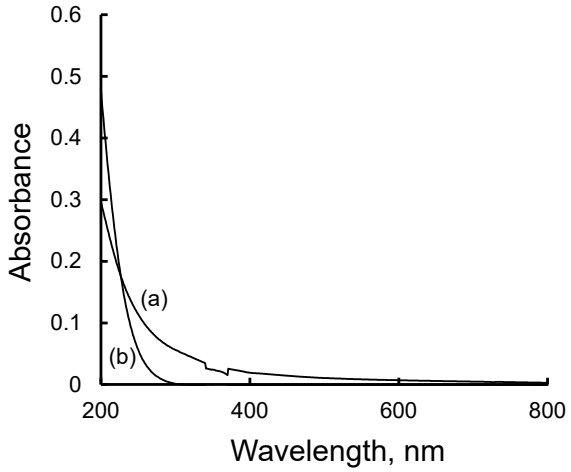

Fig. 2. Absorption spectra of (a) PtNP and (b) AgNP. The PtNP and the AgNP solutions were diluted by 1/10 and 1/500 after the preparation.

3.2. CZE measurements of the PtNP and the AgNP

Electropherograms of the PtNP and the AgNP are shown in Fig. 3. An anionic broad peak was detected with the PtNP, while both an anionic broad peak and an electrically neutral sharp peak were detected with the AgNP. Anionic broad peaks suggest that the nanoparticle solutions have successfully been prepared. The broad peaks are related with a wide range of the electrophoretic mobility, *i.e.*, wide varieties of the size and the shape of the nanoparticles [8,9,16,31]. In the comparison between the PtNP and the AgNP, the peak width is wider with the AgNP, which suggests the wide distribution in its particle size. The wide variation in the size of AgNP agrees with the TEM results in Fig. 1. Less shot signals in the electropherograms also suggest that serious aggregates or agglomerates are scarcely involved in the nanoparticle solutions. The anionic broad peak for the PtNP was detected in the pH range at 5.8 (MES−NaOH), 7.3 (HEPES−NaOH), and 9.2 (CHES−NaOH). Effective electrophoretic mobility of the anionic PtNP slightly changed at the pH range. Fast electroosmotic flow helps fast detection and relatively sharp signal of the nanoparticles, and the CHES buffer was used throughout. Broad peaks of anionic nanoparticles were continuously detected without serious shot signals of the aggregates over 50 weeks and 20 weeks for the PtNP and the AgNP, respectively. Results after 29 weeks storage for the PtNP and 18 weeks storage for the AgNP are also shown in Fig. 3. Thus, both nanoparticles were stably dispersed in an aqueous solution without any stabilizer.

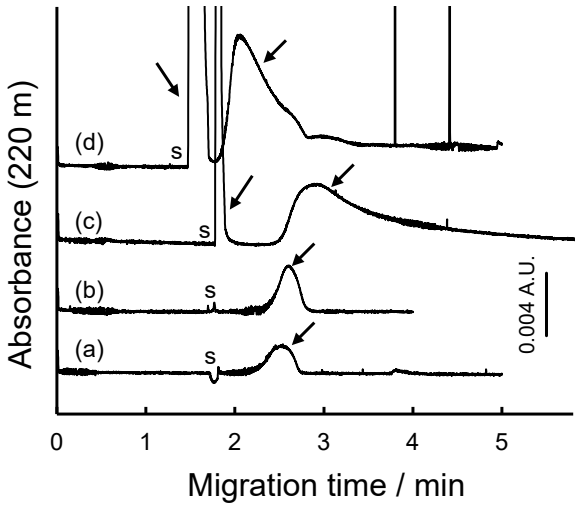

Fig. 3. Electropherograms for (a), (b) PtNP and (c), (d) AgNP. Peaks corresponding to the nanoparticles are indicated with arrows. Electropherograms (b) PtNP and (d) AgNP are the results of long-time storage after 29 weeks and 18 weeks, respectively. Separation buffer: 10 mmol L^{-1} CHES−NaOH (pH 9.2). s: solvent (electroosmotic flow). CZE conditions: 20 kV applied voltage, 50 mbar × 3 s sample injection, 220 nm detection wavelength, 25 °C capillary temperature.

3.3. Effect of addition of salt on dispersion stability of the nanoparticles

High concentrations of salt or buffer components sometimes induce the aggregation/agglomeration of nanoparticles [8,9,31], and effect of salt addition to the nanoparticle solutions was examined in this study. Halide ions are well known to form precipitates with noble metal

ions such as AgCl, and both salts of NaCl and $NaNO_3$ were examined and compared. An equal volume of the salt solution was added to an aliquot volume of the nanoparticle solution, and the mixed solution was stood for hours. Then the solution was subjected to the CZE analysis. Results on the PtNP are shown in Fig. 4. A broad peak was detected in the electropherograms with the PtNP at the migration time of around 2.4 min. Because the PtNP solution is diluted, the peak height for the PtNP is reduced from Fig. 3(a). The broad signal is detected under NaCl or $NaNO_3$ concentrations up to 5 mmol L^{-1}. Serous shot signals are detected at 10 mmol L^{-1} of the salt concentrations, while the broad peak disappeared. Generation of the shot signals suggests that the PtNP has been aggregated and agglomerated by the addition of the salts. The agglomerate would have been induced by the high slat concentrations [8,9,31].

Effect of addition of the salt was also examined with the AgNP. Results are shown in Fig. 5. A broad peak for the anionic AgNP was continuously detected without serious shot signals over NaCl or $NaNO_3$ concentrations at least up to 50 mmol L^{-1}. Another anionic broad peak was detected by the addition of $NaNO_3$ in the AgNP solution. The peak would be a formed species with added $NaNO_3$. Even when NaCl was added to the AgNP solution, any precipitate or turbidity was not observed. The results suggested that Ag^+ was scarcely contained in the AgNP solution. In our previous

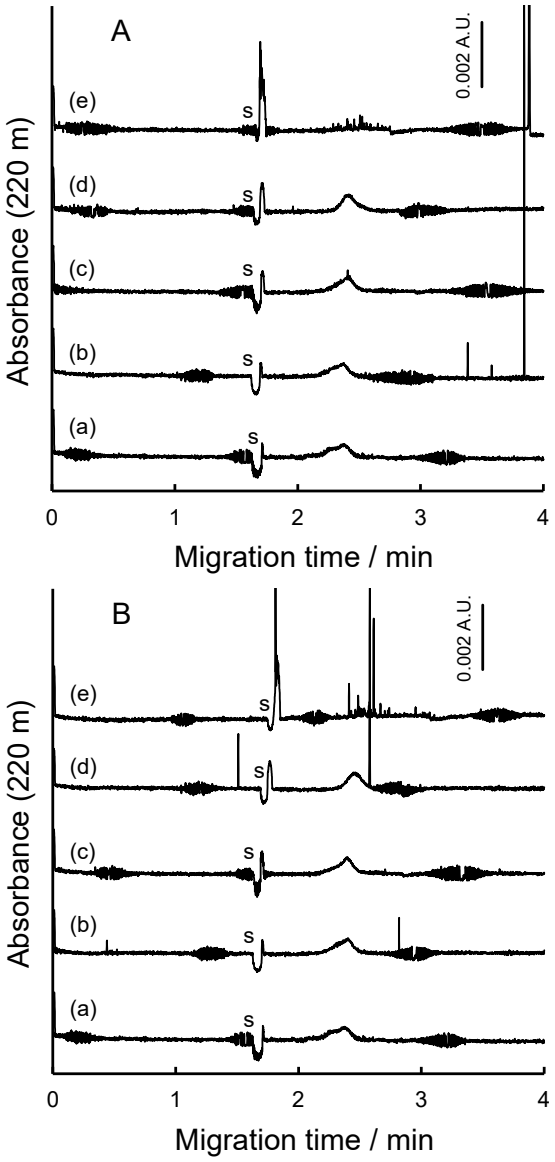

Fig. 4. Electropherograms for the PtNP in the presence of A: NaCl or B: $NaNO_3$ in the nanoparticle solution. C_{NaCl} or C_{NaNO_3}: (a) none, (b) 1 mmol L^{-1}, (c) 3 mmol L^{-1}, (d), 5 mmol L^{-1}, (e) 10 mmol L^{-1}. s: solvent (electroosmotic flow). CZE conditions: 20 kV applied voltage, 50 mbar × 3 s sample injection, 220 nm detection wavelength, 25 °C capillary temperature.

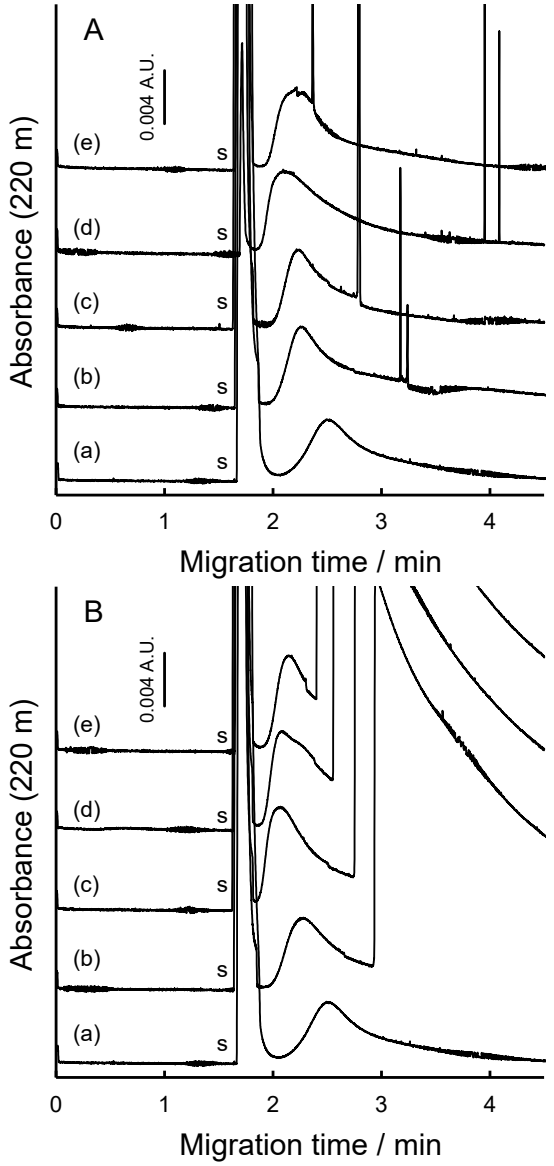

Fig. 5. Electropherograms for the AgNP in the presence of A: NaCl or B: $NaNO_3$ in the nanoparticle solution. C_{NaCl} or C_{NaNO_3}: (a) none, (b) 20 mmol L^{-1}, (c) 30 mmol L^{-1}, (d), 40 mmol L^{-1}, (e) 50 mmol L^{-1}. s: solvent (electroosmotic flow). CZE conditions: 20 kV applied voltage, 50 mbar × 3 s sample injection, 220 nm detection wavelength, 25 °C capillary temperature.

study, the AuNP prepared by the SP process stably dispersed in 30 mmol L^{-1} NaCl solution [31]. Comparing the three nanoparticles, the PtNP is the most likely to form agglomerate in the salt solution and the AgNP is the least. The PtNP is the smallest in its diameter, and its charge density would be the highest among them, and therefore, strong electrostatic interaction with the cation would have promoted the agglomeration of the PtNP.

3.4. Effect of addition of ethanol on dispersion stability of the nanoparticles

Addition of an organic solvent to an aqueous solution induces the reduction of the dielectric constant of the solvent, and electrostatic ion-ion interactions are generally developed in the solvent of the reduced dielectric constant. The developed electrostatic interactions would reduce the effective surface charge of nanoparticles by the adsorption of the counter cation, and the nanoparticles could be aggregated. We have previously reported the aggregation development of AuNP by the addition of ethanol [31]. In this study, addition of ethanol was also examined for the dispersion stability of the PtNP and the AgNP.

Effect of addition of ethanol was examined in two ways. Firstly, ethanol was added in the nanoparticle solutions, and CZE analysis was done with an ordinary aqueous separation buffer. The results are shown in Fig. 6; the nanoparticle solutions were diluted by 1/2 before the CZE measurements. A broad peak of the PtNP was successfully detected without shot signals of the aggregates at least up to 50 %(v/v) ethanol concentration (Fig. 6A), although the peak area or the peak height of the PtNP decreased a little. The result suggests that a small portion of the PtNP precipitated in the nanoparticle solution by the addition of ethanol. The migration time of the PtNP, as well as its electrophoretic mobility, did not change so much, and net charge of the anionic PtNP was almost identical in the separation buffer.

The decrease in the broad peak by the ethanol addition was much serious with AgNP (Fig. 6B). The peak area for the anionic AgNP was reduced to about 20% at 20 %(v/v) ethanol concentration, and almost diminished at 30 %(v/v) ethanol. Comparison between the PtNP and the AgNP suggests that the AgNP seriously precipitated as agglomerate in the water-ethanol mixed solvent, and concentration of the dispersed AgNP decreased.

Secondly, addition of ethanol to the separation buffer was examined. Results are shown in Fig. 7. Along with the increase in the ethanol percentage in the separation buffer, the migration of the anionic nanoparticles got slower. The longer migration time is mainly based on the suppressed speed of the electroosmotic flow. The broad peak for the anionic PtNP was normally detected with the ethanol concentrations up to 30 %(v/v). However, shot signals were detected at 40 %(v/v) ethanol concentration (Fig. 7A);

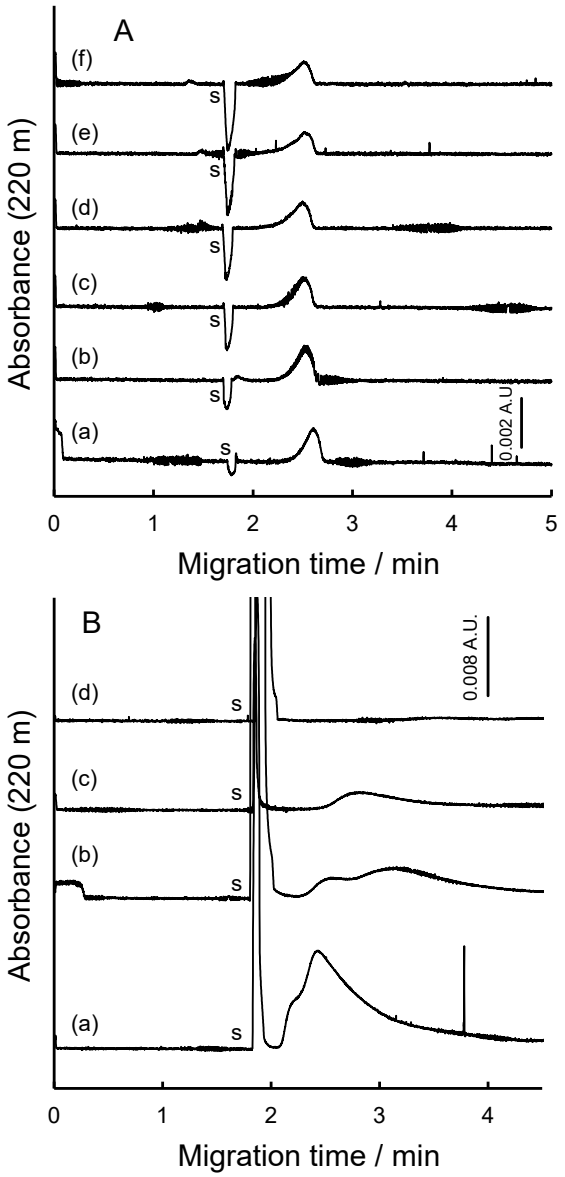

Fig. 6. Electropherograms for nanoparticles in the presence of ethanol in the nanoparticle solution. A: PtNP; B: AgNP. Concentration of ethanol: (a) none, (b) 10 %(v/v), (c) 20 %(v/v), (d) 30 %(v/v), (e) 40 %(v/v), (f) 50 %(v/v). s: solvent (electroosmotic flow). CZE conditions: 20 kV applied voltage, 50 mbar × 3 s sample injection, 220 nm detection wavelength, 25 °C capillary temperature.

aggregates/agglomerates of the anionic PtNP were formed during the electrophoresis. Developed ion-ion interactions in the solvent of reduced dielectric constant would have induced the aggregation/agglomeration of the PtNP. The AuNP prepared by the SP process stably dispersed in ethanol cosolvent up to 40 %(v/v) [31], and the dispersion stability of the PtNP is comparable to the AuNP. Results on the AgNP are shown in Fig. 7B. The migration time of the anionic AgNP got closer to the electrically neutral sharp peak, when ethanol was added in the separation buffer. The result suggests that the anionic charge of the AgNP decreased.

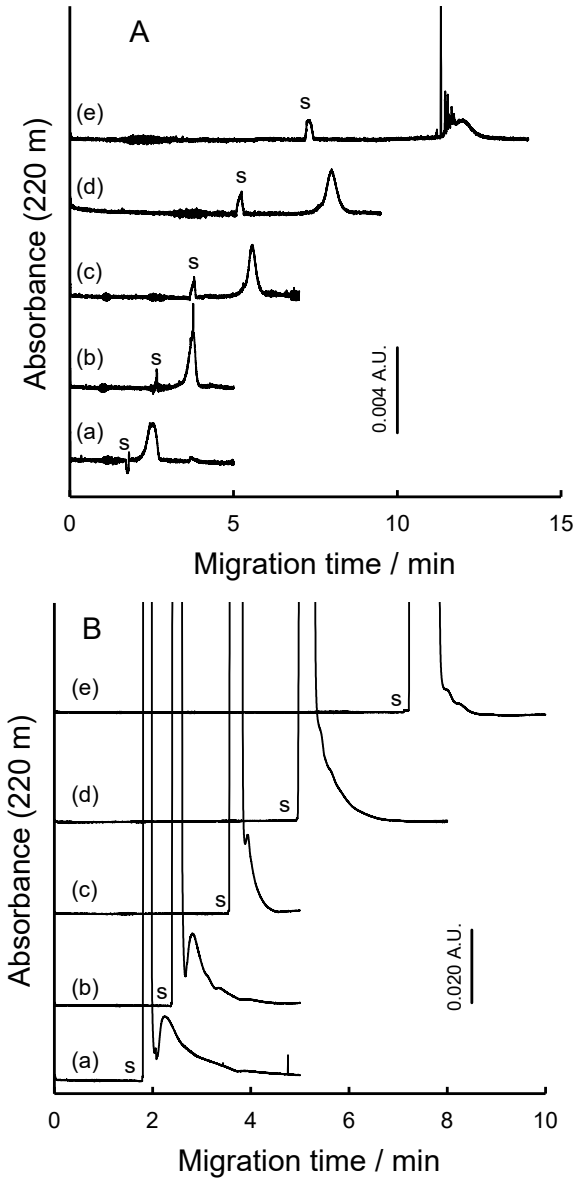

Fig. 7. Electropherograms for nanoparticles in the presence of ethanol in the separation buffer. A: PtNP; B: AgNP. Concentration of ethanol: (a) none, (b) 10 %(v/v), (c) 20 %(v/v), (d) 30 %(v/v), (e) 40 %(v/v). s: solvent (electroosmotic flow). CZE conditions: 20 kV applied voltage, 50 mbar × 3 s sample injection, 220 nm detection wavelength, 25 °C capillary temperature.

However, serious shot signals were not detected in the electropherograms at least up to 40 %(v/v) ethanol concentration in the separation buffer.

To examine the surface charge of the nanoparticles, effective electrophoretic mobility of the nanoparticles was examined. Since the electrophoretic mobility of ionic analytes depends on the viscosity of the separation buffer, the measured electrophoretic mobility of the nanoparticles, $\mu_{ep,NP}$, was standardized with that of monoanionic naphthalene-1-sulfonate ion, $\mu_{ep,NS}$, by division. Results are shown in Fig. 8. It is clearly indicated that the effective electrophoretic mobility of the nanoparticles decreased with increasing concentrations of ethanol. The result suggests that effective surface charge of the nanoparticles has decreased. It is also noted in Fig. 8 that the decrease in the effective electrophoretic mobility is more significant with the AgNP than the PtNP. The electrostatic interaction between counter cation and anionic AgNP would be stronger than that with anionic PtNP. Although the anionic nanoparticles are associable with the cations, the formed ion-associate, less-charged nanoparticles, are still dispersed in the water-ethanol solvent.

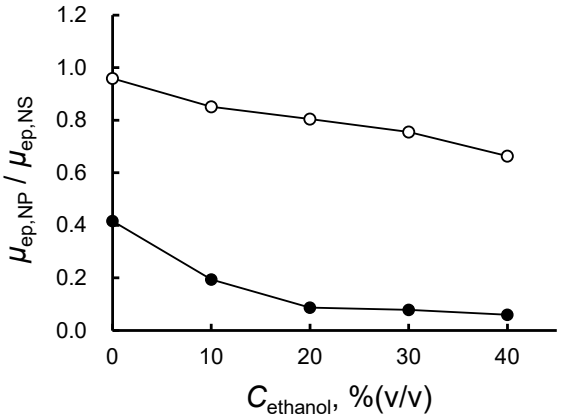

Fig. 8. Changes in the effective electrophoretic mobility of the anionic nanoparticles with increasing concentrations of ethanol in the separation buffer. The electrophoretic mobility of the nanoparticles, $\mu_{ep,NP}$, was standardized with that of naphthalene-1-sulfonate ion, $\mu_{ep,NS}$. Symbols: ○, PtNP; ●, AgNP.

4. Conclusions

In this study, solutions of PtNP and AgNP were prepared by the SP process. The nanoparticle solutions did not show visible range absorption, and thus the nanoparticle solutions were characterized by CZE. Anionic nanoparticles were detected as a broad peak with both the PtNP and the AgNP. The peak width in the electropherograms agreed with the size distribution of the nanoparticles. Dispersion stability of the PtNP and the AgNP was also evaluated in salt solutions, and the dispersion stability against salt agreed with the particle size; smaller PtNP is more likely to agglomerate. The dispersion stability was also examined with ethanol co-solvent, and decrease in the surface charge in the solution was verified with the decrease in the effective electrophoretic mobility of the nanoparticles.

References

[1] Omidfar, K.; Khorsand, F.; Azizi, M. D. *Biosens. Bioelectron.* **2013**, *43*, 336-347.
[2] Peng, Z.; Yang, H. *Nano Today* **2009**, *4*, 143-164.
[3] Le Ouay, B.; Stellacci, F. *Nano Today* **2015**, *10*, 339-354.
[4] Pryshchepa, O.; Pomastowski, P.; Buszewski, B. *Adv. Colloid Interface Sci*. **2020**, *284*, 102246.

[5] Cialla, D.; März, A.; Böhme, R.; Theil, F.; Weber, K.; Schmitt, M.; Popp, J. *Anal. Bioanal. Chem.* **2012**, *403*, 27-54.
[6] Trapiella-Alfonso, L.; Ramírez-García, G.; d'Orlyé, F.; Varenne, A. *Trends Anal. Chem.* **2016**, *84*, 121-130.
[7] Adam, V.; Vaculovicova, M. *Electrophoresis* **2017**, *38*, 2389-2404.
[8] Dziomba, S.; Ciura, K.; Kocialkowska, P.; Prahl, A.; Wielgomas, B. *J. Chromatogr. A* **2018**, *1550*, 63-67.
[9] Dziomba, S.; Ciura, K.; Correia, B.; Wielgomas, B. *Anal. Chim. Acta* **2019**, *1047*, 248-256.
[10] González Fá, A. J.; Cerutti, I.; Springer, V.; Girotti, S.; Centurión, M. E.; Di Nezio, M. S.; Pistonesi, M. F. *Chromatographia* **2017**, *80*, 1459-1466.
[11] Lin, K.-H.; Chu, T.-C.; Liu, F.-K. *J. Chromatogr. A* **2007**, *1161*, 314-321.
[12] López-Lorente, Á. I.; Soriano, M. L.; Valcárcel, M. *Microchim. Acta* **2014**, *181*, 1789-1796.
[13] Macková, H.; Oukacine, F.; Plichta, Z.; Hrubý, M.; Kučka, J.; Taverna, M.; Horák, D. *J. Colloid Interf. Sci.* **2014**, *421*, 146-153.
[14] Qin, W.; Tursen, J. *Anal. Sci.* **2009**, *25*, 333-337.
[15] Mozhayeva, D.; Engelhard, C. *Anal. Chem.* **2017**, *89*, 9767-9774.
[16] Qu, H.; Mudalige, T. K.; Linder, S. W. *Anal. Chem.* **2014**, *86*, 11620-11627.
[17] Liu, L.; He, B.; Liu, Q.; Yun, Z.; Yan, X.; Long, Y.; Jiang, G. *Angew. Chem. Int. Ed.* **2014**, *53*, 14476-14479.
[18] Franze, B.; Engelhard, C. *Anal. Chem.* **2014**, *86*, 5713-5720.
[19] Qu, H.; Mudalige, T. K.; Linder, S. W. *J. Chromatogr. A* **2016**, *1429*, 348-353.
[20] Michalke, B.; Vinković-Vrček, I. *J. Chromatogr. A* **2018**, *1572*, 162-171.
[21] Liu, F. -K.; Ko, F. -H.; Huang, P. -W.; Wu, C. -H.; Chu, T. -C. *J. Chromatogr. A* **2005**, *1062*, 139-145.
[22] Arráez Román, D.; Efremov, E.; Ariese, F.; Segura Carretero, A.; Gooijer, C. *Anal. Bioanal. Chem.* **2005**, *382*, 180-185.
[23] Nirode, W. F.; Devault, G. L.; Sepaniak, M. J. *Anal. Chem.* **2000**, *72*, 1866-1871.
[24] Přikryl, J.; Klepárník, K.; Foret, F. *J. Chromatogr. A* **2012**, *1226*, 43-47.
[25] Matsuda, N.; Nakashima, T. *IEICE Tech. Rep.* **2012**, *111*, 23-26.
[26] Matsuda, N.; Nakashima, T.; Okabe, H.; Yamada, H.; Shiroishi, H.; Nagamura, T. *Mol. Cryst. Liq. Cryst.* **2017**, *653*, 137-143.
[27] Matsuda, N.; Okabe, H.; Nagamura, T.; Uehara, M. *Mol. Cryst. Liq. Cryst.* **2019**, *686*, 63-69.
[28] Mie, Y.; Okabe, H.; Mikami, C.; Motomura, T.; Matsuda, N. *Electrochem. Commun.* **2023**, *146*, 107415.
[29] Matsuda, N.; Nakashima, T.; Kato, T.; Shiroishi, H. *Electrochim. Acta* **2014**, *146*, 73-78.
[30] Horiguchi, G.; Chikaoka, Y.; Shiroishi, H.; Kosaka, S.; Saito, M.; Kameta, N.; Matsuda, N. *J. Power Sources* **2018**, *382*, 69-76.
[31] Takayanagi, T.; Miyake, K.; Iwasaki, S.; Uehara, D.; Mizuguchi, H.; Okabe, H.; Matsuda, N. *Anal. Sci.* **2022**, *38*, 1199-1206.